Does PRODAN Possess a Planar or Twisted Charge-Transfer Excited State? Photophysical Properties of Two PRODAN Derivatives

Bethany C. Lobo and Christopher J. Abelt*

Department of Chemistry, College of William and Mary, Williamsburg, Virginia 23187-8795

Received: July 12, 2003; In Final Form: October 6, 2003

The synthesis and photochemical properties of 1-(4-methyl-1,2,3,4-tetrahydrobenzo[*f*]quinolin-8-yl)propan-1-one (**7**) and 2,2-dimethyl-1-(4-methyl-1,2,3,4-tetrahydrobenzo[*f*]quinolin-8-yl)propan-1-one **(8)** are reported. These compounds are models for PRODAN, 6-propionyl-2-(dimethylamino)naphthalene, where the dialkylamino group is forced to remain coplanar with the naphthalene ring. The Stokes shifts of **7** and **8** in various solvents are compared with those of PRODAN. The absorption and emission transitions are calculated by the AM1 semiempirical method employing a conductor-like screening model for solvent effects. The experimental and calculated solvatochroism of both model compounds are of the same magnitude as PRODAN, suggesting that all fluoresce from a planar ICT state.

I. Introduction

The development of sensors for organic and biological compounds is an important area of research. Sensors must respond to the presence of an organic substance with a signal that can be used to quantify the substance.[1] Compounds that possess an ICT (intramolecular charge transfer) state are particularly useful as sensors. Their fluorescence is modulated by the nature of their immediate environment. The environment can affect not only the fluorescence intensity but also the emission wavelength maximum and the lifetime. Our interest in these fluorophores stems from their use in the construction of fluorescent cyclodextrin chemosensors.[2−4] These systems can sense the presence of small organic substrates that are difficult to quantify otherwise.

Of the many fluorophores that have been attached to cyclodextrins, those that have a twisted intramolecular charge transfer state (TICT) are especially noteworthy.[5−7] Fluorophores that fall under this category are 5-dimethylaminonaphthalene-1-sulfonic acid (DNS) and dimethylaminobenzonitrile (DMABN, Figure 1). The lowest energy absorption in DMABN is a ^1L_b transition and it produces a planar locally excited (LE) state. Twisting 90° about the C(aryl)−N bond generates the TICT state through a surface crossing. The TICT state exhibits nearly complete electron transfer from the amino N to the cyanophenyl group. Fluorescence from the TICT state shows substantial Stokes shifts. The large charge-transfer character of the TICT state leads to high sensitivity toward certain environmental factors, especially solvent polarity. Some of the strongest evidence for the TICT model is the behavior of related model compounds that force the nitrogen lone pair to be either parallel or perpendicular to the aromatic π-system (Figure 1).[8−12] Compound **3** shows only LE emission, whereas **4** and **5** show only red-shifted CT emission. Despite the large volume of experimental evidence, the TICT model is not universally accepted.[13−16] Understanding the photophysical processes that underlie the functioning of sensors is necessary to properly interpret their signals.

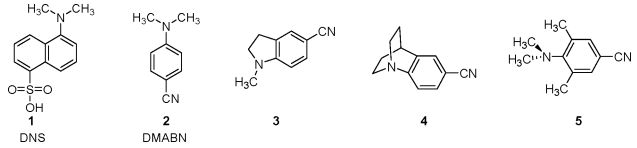

Figure 1. Structures of DNS, DMABN, and planar and twisted DMABN models **3**, **4,** and **5**.

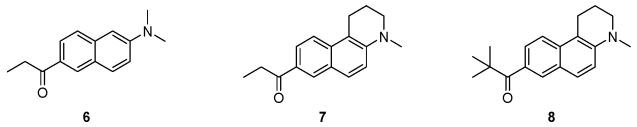

Figure 2. Structures of PRODAN, **6**, and derivatives **7** and **8**.

Since its initial synthesis by Weber and Farris in 1979,[17] PRODAN (6-propionyl-2-(dimethylamino)naphthalene, **6**, Figure 2), has found extensive use as a fluorescent probe of micropolarity. PRODAN possesses an electron-donating dimethylamino group just like DNS and DMABN. The electron-withdrawing propionyl group is positioned at maximal distance from the amino group. Transfer of electron density from the donor to the acceptor produces a substantial excited-state dipole moment that is sensitive to the polarity of the immediate environment. The similarities between PRODAN and DMABN in their structure and fluorescence properties suggest that PRODAN may also emit from a TICT state. Theoretical studies on PRODAN excited states have supported the amino-twisted geometry (TICT) as the lowest energy.[18−20] However, it was noted that this assignment was greatly dependent on the choice of the Onsager radius. The solvent stabilization by a radius of 4.6 Å favored the TICT state, whereas a slightly higher value (5.6 Å) gave the PICT (planar ICT) state as the lowest.[18] On the other hand, experimental evidence points to a PICT emitting state. Estimations of the excited-state dipole moment, either by solvatochromic studies[21−23] or by transient dielectric loss measurements,[24] show that it is only 4−7 D larger than that of the ground state. It is argued that this difference is too small for a TICT state that should show nearly full charge transfer.

We report the synthesis and photophysical properties of two PRODAN derivatives, **7** and **8** (Figure 2), where the dialkyl-

* Corresponding author. E-mail: cjabel@wm.edu.

10.1021/jp036013r CCC: $25.00
Published on Web 11/20/2003

amino group is constrained to be coplanar with the naphthalene ring. The much smaller Stokes shifts observed with similarly constrained DMABN derivatives offer critical support for the TICT model (vide supra).

II. Experimental Section

NMR spectra were obtained with a Varian Mercury VX-400 spectrometer. TLC plates (250 micron silica gel HLF from Analtech) were developed using mixture of ethyl acetate and hexanes (E/H). Combustion analyses were conducted by Desert Analytics. UV/vis absorbance measurements were performed with an Ocean Optics Chem 2000 spectrometer. Fluorescence excitation/emission studies were performed on a Perkin-Elmer LS55 luminescence spectrometer using FL WinLab software. All solvents except trifluoroethanol were spectrophotometric grade from Acros. AM1/SM5C semiempirical calculations were performed with AMPAC 6.7 from Semichem, Inc. Calculations incorporated the following keywords: AM1; C. I. = 14; singlet; qcscf; sm5c; solvnt = 'xxx'; tight; truste; micros = 0; root = 1 (or 2); gnorm = 0.2; scfcrt = 0. "Solvents" are depicted through a set of seven parameters: dielectric constant, index of refraction, H-bonding donating ability, H-bonding accepting ability, surface tension, fraction of non-H atoms that are aromatic C atoms, and fraction of non-H atoms that are halogens.

3-[(6-Bromonaphthalen-2-yl)methylamino]propionic Acid. 6-Bromo-2-methylaminonaphthalene[25] (11.14 g, 47 mmol) was dissolved in acetic acid (35 mL). Acrylic acid (15 mL, 219 mmol) was added. The mixture was heated to 110 °C with stirring for 1 h. The solution was cooled, added dropwise to cold water, and allowed to stir overnight. The resulting solid was collected and dried in vacuo giving 13.94 g (96%) of a light colored solid: R_f 0.10 (1:3 E/H); ^{1}H NMR ($CDCl_3$) δ 7.70 (s, 1 H), 7.47 (d, J = 9.0 Hz, 1 H), 7.39 (d, J = 8.7 Hz, 1 H), 7.33 (d, J = 8.7 Hz, 1 H), 7.30 (d, J = 9.0 Hz, 1 H), 6.76 (s, 1 H), 3.63 (t, J = 7.1 Hz, 2 H), 2.89 (s, 3 H), 2.53 (t, J = 7.1 Hz, 2 H); ^{13}C NMR ($CDCl_3$) 178.5, 146.8, 133.6, 129.7, 129.6, 128.4, 128.2, 119.2, 117.3, 115.8, 107.2, 49.0, 38.9, 32.0. This material was used without further purification in the next step.

8-Bromo-4-methyl-3,4-dihydro-2*H*-benzo[f]quinolin-1-one. 3-[(6-Bromonaphthalen-2-yl)methylamino]propionic acid (13.84 g, 48 mmol) was combined with polyphosphoric acid (150 mL). The mixture was heated to 150 °C with stirring for 90 min. It was poured into stirring cold water and allowed to precipitate fully from solution. The product was collected and dried in vacuo leaving 10.76 g (80%) of a brown solid: R_f 0.14 (1:3 E/H); ^{1}H NMR ($CDCl_3$) 9.38 (d, J = 9.3 Hz, 1 H), 7.75 (d, J = 2.4 Hz, 1 H), 7.69 (d, J = 9.3 Hz, 1 H), 2.77 (t, J = 3.9 Hz, 2 H), 7.54 (dd, J = 2.4, 9.4 Hz, 1 H), 7.01 (d, J = 9.4 Hz, 1 H), 3.59 (t, J = 7.3 Hz, 2 H), 3.17 (s, 3 H), 2.78 (t, J = 7.3 Hz, 2 H); ^{13}C NMR ($CDCl_3$) 193.9, 154.0, 135.8, 132.6, 131.6, 130.1, 128.4, 127.6, 116.7, 116.2, 110.0, 51.5, 40.6, 39.4. This material was used in the next step without further purification.

8-Bromo-4-methyl-1,2,3,4-tetrahydrobenzo[*f*]quinoline. 8-Bromo-4-methyl-3,4-dihydro-2*H*-benzo[*f*]quinolin-1-one (10.76 g, 36 mmol) was dissolved in diethylene glycol (140 mL). Hydrazine monohydrate (5.0 g, 100 mmol) and KOH (5.0 g, 89 mmol) were added. The solution was heated to reflux (ca. 200 °C) with stirring for 90 min. The reaction mixture was allowed to cool to 80 °C and then was added dropwise to stirring cold water. The precipitate was collected and dried in vacuo leaving 8.96 g (88%) which was used in the next step. A sample was sublimed for analysis: mp 112−114 °C, R_f 0.69 (1:3 E/H); ^{1}H NMR ($CDCl_3$) δ 7.80 (d, J = 2.0 Hz, 1 H), 7.60 (d, J = 9.1 Hz, 1 H), 7.50 (d, J = 9.2 Hz, 1 H), 7.44 (dd, J = 2.0, 9.1 Hz, 1 H), 7.10 (d, J = 9.2 Hz, 1 H), 3.26 (m, 2H), 3.03 (m, 2 H), 3.00 (s, 3 H), 2.13 (m, 2 H); ^{13}C NMR ($CDCl_3$) δ 144.9, 131.6, 130.4, 129.4, 128.2, 126.4, 123.6, 116.3, 115.0, 113.6, 51.5, 40.4, 23.8, 22.3. Anal. Calcd for $C_{14}H_{14}NBr$: C, 60.89; H, 5.11; N, 5.07. Found: C, 60.63; H, 4.99; N, 5.01.

8-Cyano-4-methyl-1,2,3,4-tetrahydrobenzo[*f*]quinoline. 8-Bromo-4-methyl-1,2,3,4-tetrahydrobenzo[*f*]quinoline (4.98 g, 18 mmol) was dissolved in freshly distilled dimethylacetamide (125 mL). CuCN (9.21 g, 103 mmol) was added, and the solution was heated to reflux for 1 h under N_2. Most of the solvent was removed by distillation. The remaining solution was poured into stirring cold H_2O (500 mL). The product was collected and dried in vacuo. The solid was ground together with basic Al_2O_3, placed in a Soxhlet thimble, and extracted with CH_2Cl_2 for 48 h. The extract was concentrated in vacuo, and the resulting solid was dried in vacuo leaving 3.2 g (80%). A sample was sublimed for analysis: mp 116−118 °C, R_f 0.56 (1:3 E/H); ^{1}H NMR ($CDCl_3$) δ 8.00 (d, J = 1.7 Hz, 1 H), 7.73 (d, J = 8.8 Hz, 1 H), 7.60 (d, J = 9.2 Hz, 1 H), 7.48 (dd, J = 1.7, 8.8 Hz, 1 H), 7.12 (d, J = 9.2 Hz, 1 H), 3.34 (m, 2 H), 3.05 (s, 3 H), 3.02 (m, 2 H), 2.12 (m, 2 H); ^{13}C NMR ($CDCl_3$) δ 147.1, 134.4, 128.1, 126.9, 125.9, 125.6, 122.4, 120.3, 116.2, 112.7, 106.0, 51.3, 39.9, 23.6, 22.0. Anal. Calcd for $C_{15}H_4N_2 \cdot (H_2O)_{0.2}$: C, 79.76; H, 6.43; N, 12.40. Found: C, 79.97; H, 6.45; N, 12.15.

1-(4-Methyl-1,2,3,4-tetrahydrobenzo[*f*]quinolin-8-yl)propan-1-one. 8-Cyano-4-methyl-1,2,3,4-tetrahydrobenzo[*f*]quinoline (2.42 g, 11 mmol) was dissolved in THF (30 mL). Ethylmagnesium chloride (6 mL, 2 M in THF, 12 mmol) and CuBr (0.09 g, 0.63 mmol) were added, and the mixture was heated to reflux under N_2 for 24 h. The reaction was cooled and the solvent was removed in vacuo. H_2O and HCl (20 mL each) were added, and the mixture was heated at reflux for another 24 h. The reaction was cooled, and the solution was neutralized with $NaHCO_3$. The aqueous layer was extracted with CH_2Cl_2 (3 × 150 mL). The organic layer was washed with H_2O, dried over $MgSO_4$, and concentrated in vacuo leaving 2.37 g (85%). A portion of this product was dissolved in acetone, filtered through a plug of basic Al_2O_3, and precipitated from H_2O. The precipitate was sublimed under vacuum giving a yellow solid: mp 119−120 °C, R_f 0.55 (1:3 E/H); ^{1}H NMR ($CDCl_3$) δ 8.31 (d, J = 1.9 Hz, 1 H), 7.96 (dd, J = 1.9, 9.0 Hz, 1 H), 7.73 (d, J = 9.2 Hz, 1 H), 7.69 (d, J = 9.0 Hz, 1 H), 7.10 (d, J = 9.2 Hz, 1 H), 3.29 (m, 2 H), 3.09 (q, J = 7.4 Hz, 2 H), 3.06 (m, 2 H), 3.05 (s, 3 H), 2.13 (m, 2 H), 1.26 (t, J = 7.4 Hz, 3 H); ^{13}C NMR ($CDCl_3$) δ 200.6, 146.6, 135.3, 130.6, 129.9, 129.4, 125.5, 124.7, 121.7, 115.6, 113.0, 51.4, 40.1. Anal. Calcd for $C_{17}H_{19}NO$: C, 80.60; H, 7.56; N, 5.53. Found: C, 80.81; H, 7.28; N, 5.77.

2,2-Dimethyl-1-(4-methyl-1,2,3,4-tetrahydrobenzo[*f*]quinolin-8-yl)propan-1-one. The reactants, their quantities, and procedure are identical to those above except that *tert*-butylmagnesium chloride (6.4 mL, 2 M in THF, 12.8 mmol) was used. This reaction gave 2.69 g (87%). Purification was as above: mp 150−152 °C, R_f 0.67 (1:3 E/H); ^{1}H NMR ($CDCl_3$) δ 8.22 (d, J = 1.9 Hz, 1 H), 7.86 (dd, J = 1.9, 9.0 Hz, 1 H), 7.71 (d, J = 9.0 Hz, 1 H), 7.67 (d, J = 9.2 Hz, 1 H), 7.10 (d, J = 9.2 Hz, 1 H), 3.31 (m, 2 H), 3.06 (m, 2 H), 3.04 (s, 3 H), 2.13 (m, 2 H), 1.44 (s, 9 H); ^{13}C NMR ($CDCl_3$) δ 207.4, 146.2, 134.3, 130.6, 130.3, 129.1, 126.1, 125.4, 121.2, 115.6, 113.0, 51.5, 44.4, 40.2, 28.9, 23.7, 22.3. Anal. Calcd for $C_{19}H_{23}NO \cdot (H_2O)_{0.2}$: C, 80.07; H, 8.28; N, 4.91. Found: C, 79.88; H, 8.27; N, 5.11.

SCHEME 1: Synthesis of PRODAN Derivatives 7 and 8

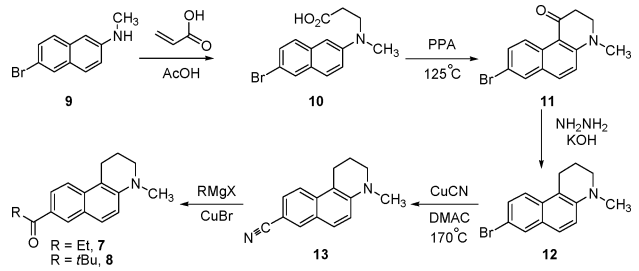

III. Results and Discussion

Synthesis. Compounds **7** and **8** are prepared by the sequence of reactions shown in Scheme 1. This route is quite different than the published route for PRODAN where the ketone moiety is introduced first.[17] All of the reactions are straightforward transformations that proceed in reasonable yield without significant side reactions. Beginning the sequence with the *N*-methyl derivative **9** obviates the need for selective *N*-alkylation later. It also allows excess acrylic acid to be used in the Michael addition (step 1). The intramolecular Friedel−Crafts acylation (step 2) shows complete regioselectivity for the α-naphthyl position. A Wolff−Kishner reduction (step 3) followed by a Rosenmund von Braun cyanation[26] (step 4) gives the nitrile **13**. The nitrile allows for the synthesis of different ketones by varying the structure of the Grignard reagent used in the next step. It is necessary to catalyze the Grignard reaction with Cu(I)Br to drive it to completion, especially for the preparation of the *tert*-butyl derivative **8**.[27]

Photophysical Studies. The photophysical behavior of **7** and **8** is examined in a series of solvents that span a wide range in polarity. The absorption spectra of **7** and **8** (Figure 3) are similar to those of PRODAN. All spectra show a broad, unsymmetrical band centered around 370 nm, except those with cyclohexane solvent. The bands become broader with increasing solvent polarity. The spectra with trifluoroethanol solvent show a significant shoulder around 390 nm. Similar behavior in PRODAN is attributed to the presence of two closely spaced $\pi \rightarrow \pi^*$ transitions[18,20,28,29] and to specific solute−solvent interactions with the protic solvents.[30]

The emission spectra of **7** and **8** are also similar to those of PRODAN. Spectra with cyclohexane solvent show two maxima, whereas in more polar solvents only one maximum is apparent. Both **7** and **8** show large Stokes shifts in polar solvents. With methanol and trifluoroethanol as the solvent the fluorescence bands are red-shifted above 500 nm. The fluorescence intensity decreases with increasing solvent polarity. In fact, the long wavelength emission with trifluoroethanol solvent is reduced almost to a shoulder.

TABLE 1: Peak Absorption (nm), Peak Emission (nm), and Stokes Shifts (cm^{-1}) for 6,[21] 7, and 8

	6			**7**			**8**		
solvent	abs	em	Stokes	abs	em	Stokes	abs	em	Stokes
cyclohexane	343	392	3904	355	409	3657	353	407	3739
toluene	349	416	4658	362	430	4348	361	432	4537
chlorobenzene	354	425	4757	366	441	4657	366	445	4858
$CHCl_3$	355	434	5151	368	453	5143	367	452	5109
ethyl acetate	348	430	5491	361	446	5310	359	448	5564
CH_2Cl_2	354	440	5219	368	456	5242	364	458	5632
2-butanone	352	443	5814	364	456	5556	362	457	5711
CH_3CN	352	456	6407	365	466	5952	362	465	6074
DMSO	358	464	6117	370	474	5892	369	472	5908
^{i}PrOH	360	480	6817	373	495	6580	368	494	6927
MeOH	361	503	7465	375	513	7206	368	512	7638
CF_3CH_2OH	370	518	8204	371	523	7794	356	515	8691

The absorption and emission properties of **6**, **7,** and **8** are summarized in Table 1. This tabulation shows that both the absorption and emission maxima of **6** are uniformly lower than those of **7** and **8** by an average of 12 nm. This effect can be attributed to the extra fused ring structure present in **7** and **8**. It is also interesting to note that **8** behaves similarly as **6** and **7** in light of the fact that the carbonyl group is forced to twist out of the molecular plane (vide infra).

A more relevant comparison with PRODAN is the relative magnitude of the solvatochroism as determined by the Lippert-Mataga equation (eq 1).

$$\tilde{\nu}_a - \tilde{\nu}_{em} = \frac{2}{hca^3}(\mu^* - \mu)^2 \Delta f + \text{const} \qquad (1)$$

where

$$\Delta f = \frac{\epsilon - 1}{2\epsilon + 1} - \frac{n^2 - 1}{2n^2 - 1}$$

Plots of the Stokes shifts as a function of the solvent polarity factor Δf are shown in Figure 5. Only the data involving the aprotic solvents are shown because application of this analysis with solvents where specific solute−solvent interactions are present is not appropriate.[23,31,32] The slope of the best-fit line is related to the dipole moment change between the ground and excited states ($\mu^* - \mu$). The slopes of all three lines are essentially identical: 6690, 6550, and 6610 cm^{-1} for **6**, **7,** and **8**, respectively. The differences in dipole moments amount to 7 D for all three.

Theoretical Calculations. The absorption and emission spectra for **6**, **7,** and **8** are calculated by using the AM1 semiempirical method by optimization of the first two singlet roots. Although this method is approximate, it allows for large

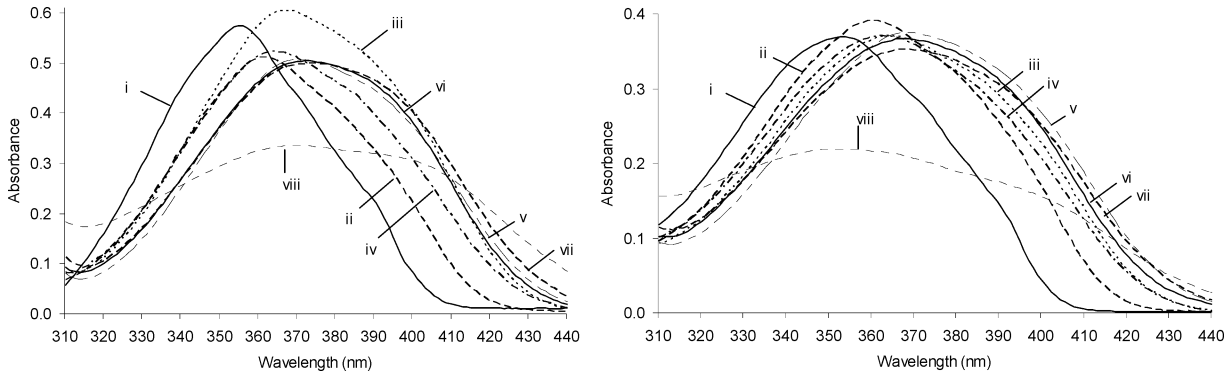

Figure 3. Absorption spectra of **7** (left) and **8** (right) in various solvents: (i) cyclohexane, (ii) toluene, (iii) CH_2Cl_2, (iv) CH_3CN, (v) DMSO, (vi) IPrOH, (vii) CH_3OH, and (viii) CF_3CH_2OH.

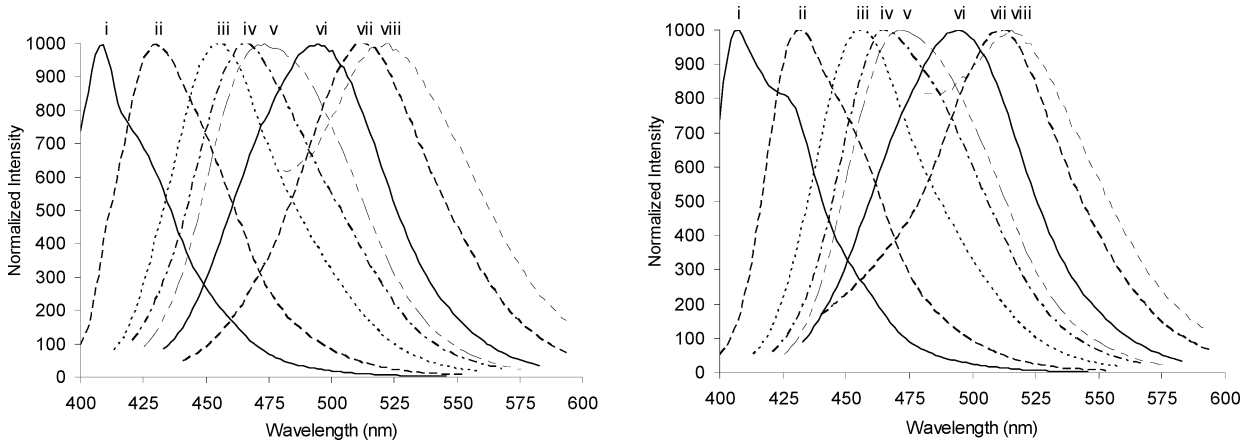

Figure 4. Emission spectra of **7** (left) and **8** (right) in various solvents: (i) cyclohexane, (ii) toluene, (iii) CH_2Cl_2, (iv) CH_3CN, (v) DMSO, (vi) IPrOH, (vii) CH_3OH, and (viii) CF_3CH_2OH.

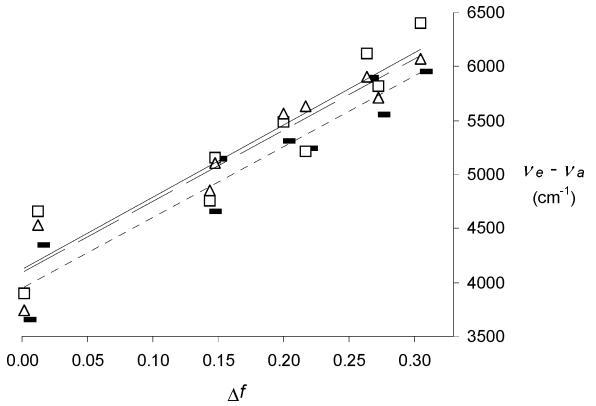

Figure 5. Lippert-Mataga plots for **6** (□, —), **7** (-, - - -) and **8** (△, — — —).

CI level calculations that incorporate the effect of solvent. The solvent is modeled as a dielectric continuum using a conductor-like screening (COSMO) approach. The solvent and solute are allowed to polarize each other, and the calculation is iterated to a self-consistent reaction field. The CI level for these calculations was set to 14 to include the 12 π-MO's and lone pair MO's on N and O. Parusel found that AM1/CISD results approach the quality of DFT/SCI calculations.[18] The ground and excited-state structures of **6** and **7** have planar dialkyl amino groups. The carbonyl group is coplanar with the naphthalene ring and can adopt two orientations. To be consistent with previous PRODAN calculations, only structures where the C5—C6—C═O dihedral angle is about 180° are considered. As it turns out, the two conformational isomers have similar energies and spectroscopic properties. The carbonyl group in **8**, on the other hand, is forced to twist out of plane by nearly 90° in both the ground and excited states. In the ground state the amino group in **8** is slightly pyramidal, while in the excited state it is planar.

To make sure that the ring fusion enforces the coplanarity of the amino group, the energies of the first excited state in acetonitrile are calculated for a series of increasing twist angles. The amino N is not allowed to pyramidalize in these calculations. Pyramidalization shifts the peak emission to much shorter wavelengths in contrary to experiment. The plot of energy vs twist angle is shown in Figure 6. As expected, the curve is concave up, indicating that further twisting becomes much more difficult as the twist angle increases. Surprisingly, the calculated emission bands decreases from 480 to 470 nm as the twist angle increases to 35° and then it remains relatively constant.

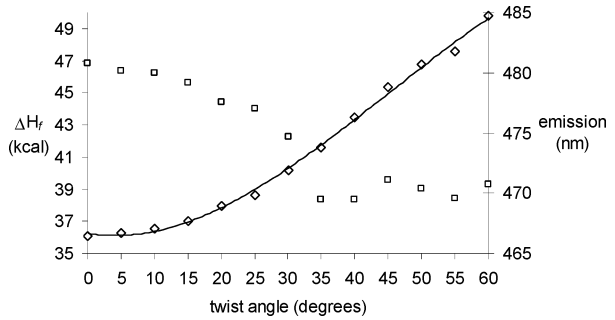

Figure 6. Calculated heats of formation (◇) and peak wavelengths of the emission bands (□) of the first excited state of **7** as a function of the C1—C2—N—C_{ring} dihedral angle in acetonitrile.

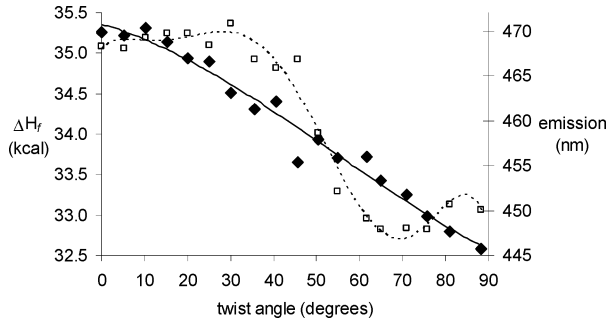

Figure 7. Calculated heats of formation (◆) and peak wavelengths of the emission bands (□) of the first excited state of **8** as a function of the C7—C6—C═O dihedral angle in acetonitrile.

The rotation of the *tert*-butylcarbonyl group shows the opposite trend (Figure 7). The energy minimum for the excited state is at the perpendicular orientation. The energy difference between the perpendicular and planar conformations is only slightly more than 3 kcal/mol. While the change in energy with twist angle is monotonic, the emission wavelength shows a sinusoidal dependence. The emission maximum drops sharply at angles above 45° where the conjugation between the carbonyl and naphthalene is effectively broken. The predicted energy minimum for the perpendicular geometry may be an artifact of the AM1 method. The AM1 method is known to overemphasize steric interactions relative to π-interactions.[33] Given that **7** and **8** behave similarly in both their absorption and emission properties, it is likely that the *tert*-butyl group is not twisted enough to significantly decouple the carbonyl and aromatic π-systems. Examination of the frontier MO's shows that the carbonyl group comprises only about 10% of the lowest two

TABLE 2: Calculated Peak Absorption and Peak Emission Bands (nm), *x,y*-Components of the Transition Moment (au) and Oscillator Strengths (*f*) for 6, 7, and 8 in Various Solvents

		6				**7**				**8**				**8**[b]			
	solv[a]	band	x	y	f	band	x	y	f	band	x	y	f	band	x	y	f
								Absorption[c]									
S_0–S_1	i	369	−13	23	1	400	−5	71	4	382	−20	47	2	380	−20	44	2
	ii	371	−10	26	1	403	−1	77	5	387	−19	41	2	383	−21	40	2
	iii	374	−4	28	1	409	18	99	8	381	−22	48	2	382	−18	47	2
	iv	375	9	47	2	409	20	100	8	382	−22	49	2	383	−17	49	2
	v	376	10	49	2	414	21	101	8	383	−22	49	2	383	−17	49	2
S_0–S_2	i	353	76	126	19	381	79	129	18	344	45	113	13	356	56	120	15
	ii	355	77	126	19	384	81	125	18	349	41	113	13	354	55	122	15
	iii	360	84	129	20	391	89	115	16	350	54	119	15	360	67	123	17
	iv	363	89	124	19	391	96	117	18	347	57	119	15	361	71	124	17
	v	365	89	124	19	394	95	116	17	348	57	119	15	362	71	124	17
								Emission[c]									
S_1–S_0	i	414	9	77	4	438	−5	75	4	436	−24	57	3	432	−15	63	3
	ii	416	6	70	4	443	−3	85	5	438	−24	58	3	435	−15	64	3
	iii	447	60	131	14	470	38	139	13	446	−22	60	3	457	−15	78	4
	iv	454	66	134	15	481	60	157	18	450	−22	61	3	464	-13	80	4
	v	454	67	135	15	481	61	158	18	450	-22	61	3	464	−13	81	4

[a] Solvents: (i) cyclohexane; (ii) toluene; (iii) CH_2Cl_2; (iv) CH_3CN; (v) DMSO. [b] C7—C6—C=O constrained at 45°. [c] *x,y*-components and oscillator strengths $\times 10^2$.

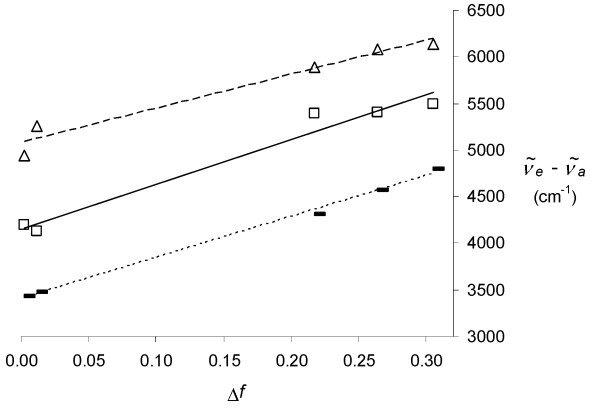

Figure 8. Lippert-Mataga plot for calculated Stokes shifts for **6** (□, —), **7** (-, - - -) and **8** (△, — — —).

LUMO's, suggesting that its partial rotation will not have a dramatic effect on the spectroscopic properties.

The calculated absorption and emission transitions for **6**, **7,** and **8** are shown in Table 2. In line with previous theoretical studies,[18,19,28,29] all show two closely spaced long wavelength absorption transitions. The lowest energy transition (S_0–S_1) is weaker than the S_0–S_2 transition. For PRODAN it is 10−30 times weaker, whereas for **7** and **8** it is 2−8 times weaker. The calculations did not show a twinning of the second transition that did a previous study.[20] Both bands show significant long-axis polarization, but the S_0–S_2 transition shows relatively more short-axis polarization than does the S_0–S_1 transition. Assuming that the absorption maximum is determined by the stronger S_0–S_2 transition, the calculations overestimate the wavelength of the observed bands by an average of 8 and 24 nm for **6** and **7**, and they underestimate those for **8** by 4 nm for the 45°-twisted carbonyl structure (14 nm for the perpendicular carbonyl structure). For the emission bands, the calculations generally underestimate the wavelength, but they are in better agreement than the absorption numbers. In fact, if the cyclohexane data are excluded, then the average difference is 5, 12, and 3 nm, respectively. Finally, the calculations show that the nature of the emission band changes with increasing solvent polarity with **6** and **7**. With CH_2Cl_2, CH_3CN, and DMSO the polarization and oscillator values resemble those of the S_0–S_2 absorption and not the S_0–S_1 transition.

The data in Table 2 are used to make the Lippert-Mataga plots shown in Figure 8. The Stokes shift is calculated from the difference in energy between the S_0–S_2 absorption band and the S_0–S_1 emission band. For the *tert*-butyl derivative **8** the energies for the 45°-twisted carbonyl structures are used. The unusually large shifts with **8** result from the high-energy S_0–S_2 absorption bands. The slopes of the best fit lines for **6**, **7,** and **8** are 4800, 4400, and 3600 cm^{-1}, respectively. These values are approximately two-thirds of the experimental values. In comparison, the slope of the plot for PRODAN with TICT emission (i.e., where the dimethylamino group is constrained to be perpendicular to the naphthalene ring) is calculated to be 13 000 cm^{-1} (Supporting Information).

IV. Conclusions

There are two levels of conclusions that can be drawn from the experimental and theoretical data. The first is a more conservative but more definitive statement. With the explicit assumption that **7** and **8** are reasonable models of PRODAN, the data show that twisting about the C(aryl)−N bond is not necessary for the solvatochromic behavior in PRODAN. The second conclusion is that PRODAN emits from a PICT state. This conclusion is more tentative, and it requires an N-TICT model compound that shows different photophysical behavior than PRODAN.

The behavior of **8** speaks to whether the emission in **6** and **7** occurs from a twisted propionyl group (O-TICT). The calculations suggest that the effect of a twisted carbonyl group is to shift both the $S_0 \rightarrow S_2$ absorption and the $S_1 \rightarrow S_0$ emission to higher energies. Experimental results show that there is no significant different between these bands in **7** and **8**. There are two possible interpretations of these data. First is that the emissive state for all three is O-TICT. Second is that partial twisting of the carbonyl group does not significantly alter the energy of S_0 and S_1.

Acknowledgment is made to the donors of the Petroleum Research Fund, administered by the American Chemical Society, for support of this research.

Supporting Information Available: Excitation and ^1H NMR spectra of **7** and **8** and a Lippert-Mataga plot for N-TICT

PRODAN. This material is available free of charge via the Internet at http://pubs.acs.org.

References and Notes

(1) Czarnik, A. W. Supramolecular chemistry, fluorescence, and sensing. In *Fluorescent Chemosensors for Ion and Molecule Recognition*; ACS Symposium Series 538; Anerican Chemical Society: Washington, DC, 1993; pp 1−9.

(2) Ueno, A.; Matsumura, S.; Kanai, T.; Mihara, H. Chemosensors of modified cyclodextrins for detecting molecules. In *Proceedings of the International Symposium Cyclodextrins, 9th*; 1999; pp 231−234.

(3) Ueno, A.; Ikeda, H.; Wang, J. Signal transduction in chemosensors of modified cyclodextrins. In *Chemosensors of Ion and Molecule Recognition*, *NATO ASI Series, Series C: Math. Phys. Sci.*; 1997; Vol. 492, pp 105−119.

(4) Ueno, A. *Supramol. Sci.* **1996**, *3*, 31−36.

(5) Rettig, W. Photoinduced charge separation via twisted intramolecular charge transfer states. In *Top. Curr. Chem.* **1994,** *169*, pp 253−99.

(6) Rettig, W.; Lapouyade, R. Fluorescence probes based on twisted intramolecular charge transfer (TICT) states and other adiabatic photoreactions. In *Top. Fluoresc. Spectrosc.* **1994,** *4*, 109−49.

(7) Rettig, W. *Angew. Chem., Int. Ed. Engl.* **1986**, *25*, 969−86.

(8) Okada, T.; Uesugi, M.; Koehler, G.; Rechthaler, K.; Rotkiewicz, K.; Rettig, W.; Grabner, G. *Chem. Phys.* **1999**, *241*, 327−337.

(9) Koehler, G.; Rechthaler, K.; Grabner, G.; Luboradzki, R.; Suwinska, K.; Rotkiewicz, K. *J. Phys. Chem. A* **1997**, *101*, 8518−8525.

(10) Wermuth, G.; Rettig, W. *J. Phys. Chem.* **1984**, *88*, 2729−2735.

(11) Rotkiewicz, K.; Rubaszewska, W. *J. Lumin.* **1982**, *27*, 221−230.

(12) Grabowski, Z. R.; Rotkiewicz, K.; Siemiarczuk, A.; Cowley, D. J.; Baumann, W. *Nouv. J. Chim.* **1979**, *3*, 443−54.

(13) Zachariasse, K. A. *Chem. Phys. Lett.* **2000**, *320*, 8−13.

(14) Il'Ichev, Y. V.; Kuehnle, W.; Zachariasse, K. A. *J. Phys. Chem. A* **1998**, *102*, 5670−5680.

(15) Zachariasse, K. A.; Grobys, M.; von der Haar, T.; Hebecker, A.; Il'ichev, Y. V.; Morawski, O.; Rueckert, I.; Kuehnle, W. *J. Photochem. Photobiol. A: Chem.* **1997**, *105*, 373−383.

(16) Zachariasse, K. A.; von der Haar, T.; Leinhos, U.; Kuehnle, W. *J. Inf. Rec. Mater.* **1994**, *21*, 501−6.

(17) Weber, G.; Farris, F. J. *Biochemistry* **1979**, *18*, 3075−8.

(18) Parusel, A. B. J.; Nowak, W.; Grimme, S.; Koehler, G. *J. Phys. Chem. A* **1998**, *102*, 7149−7156.

(19) Parusel, A. B. J.; Schneider, F. W.; Kohler, G. *THEOCHEM* **1997**, *398*−*399*, 341−346.

(20) Ilich, P.; Prendergast, F. G. *J. Phys. Chem.* **1989**, *93*, 4441−4447.

(21) Catalan, J.; Perez, P.; Laynez, J.; Garcia Blanco, F. *J. Fluor.* **1991**, *1*, 215−23.

(22) Balter, A.; Nowak, W.; Pawelkiewicz, W.; Kowalczyk, A. *Chem. Phys. Lett.* **1988**, *143*, 565−70.

(23) Kawski, A. *Z. Naturforsch.* **1999**, *54a*, 379−381.

(24) Samanta, A.; Fessenden, R. W. *J. Phys. Chem. A* **2000**, *104*, 8972−8975.

(25) Balo, C.; Fernandez, F.; Garcia-Mera, X.; Lopez, C. *Org. Prep. Proc. Int.* **2000**, *32*, 367−372.

(26) Ellis, G.; Romney-Alexander, T. *Chem. Rev.* **1987**, *87*, 779−794.

(27) Weiberth, F.; Hall, S. *J. Org. Chem.* **1987**, *52*, 3901−3904.

(28) Parusel, A. *J. Chem. Soc., Faraday Trans.* **1998**; *94*, 2923−2927.

(29) Nowak, W.; Adamczak, P.; Balter, A.; Sygula, A. *THEOCHEM* **1986**, *32*, 13−23.

(30) Chapman, C. F.; Fee, R. S.; Maroncelli, M. *J. Phys. Chem.* **1995**, *99*, 4811−4819.

(31) Cerezo, F. M.; Rocafort, S. C.; Sierra, P. S.; Garcia-Blanco, F.; Oliva, C. D.; Sierra, J. C. *Helv. Chim. Acta* **2001**, *84*, 3306−3312.

(32) Zurawsky, W. P.; Scarlata, S. F. *J. Phys. Chem.* **1992**, *96*, 6012−16.

(33) Ahn, N. T.; Frison, G.; Solladie-Cavallo, A.; Metzner, P. *Tetrahedron* **1998**, *54*, 12841−12852.